Chapter 8
New Insights into Metabolic Regulation from Hyperpolarized ^{13}C MRS/MRI Studies

A. Dean Sherry and Craig R. Malloy

Abbreviations

GNG	Gluconeogenesis
HP	Hyperpolarized
NMR	Nuclear magnetic resonance
PC	Pyruvate carboxylase
PDH	Pyruvate dehydrogenase
PEP	Phosphoenolpyruvate
PEPCK	Phosphoenolpyruvate carboxykinase
TCA cycle	Tricarboxylic acid cycle or Krebs cycle

A. D. Sherry (✉)
Advanced Imaging Research Center and the Department of Radiology, University of Texas Southwestern Medical Center, Dallas, TX, USA

Department of Chemistry and Biochemistry, University of Texas at Dallas, Richardson, TX, USA
e-mail: Dean.Sherry@utsouthwestern.edu

C. R. Malloy
Advanced Imaging Research Center and the Department of Radiology, University of Texas Southwestern Medical Center, Dallas, TX, USA

Department of Internal Medicine, University of Texas Southwestern Medical Center, Dallas, TX, USA

Veterans Affairs North Texas Health Care System, Dallas, TX, USA

T. Jue, D. Mayer (eds.), *Dynamic Hyperpolarized Nuclear Magnetic Resonance*, Handbook of Modern Biophysics, https://doi.org/10.1007/978-3-030-55043-1_8

8.1 Introduction

Disruption of intermediary metabolism plays a central role in many high-impact diseases such as cancer, diabetes, heart disease, and genetic disorders. The growing appreciation of complex interactions among disease, genetics, intermediary metabolism, and cell signaling has reawakened intense interest in the classical metabolic pathways. Although the details of transporter kinetics and enzyme regulation continue to be refined, the focus of metabolic research is no longer the discovery of enzymes. In fact, the details of pathways are well described in maps and databases with extensive information about genes, enzymes, substrates, products, and cell compartments. Instead, the focus of research has shifted to a better understanding of the integrated function of these systems. The detailed mechanism of the Warburg phenomenon, for example, is only beginning to emerge. The role of intermediates in common metabolic pathways also continues to be refined. The last two decades have seen the surprising development of new concepts such as "oncometabolites," small molecules such as fumarate, succinate, and 2-hydroxyglutarate that are thought to drive the development of some malignancies [1, 2].

Recent studies of intermediary metabolism have emphasized measurement of gene transcripts, enzyme expression, and large-scale metabolomics to assess relative changes in the concentration of small metabolites. Although these methods provide considerable insight, information about flux in specific pathways and reactions is essential to link metabolism and the physiology of functioning tissue. Historically, fluxes were measured in individual pathways using appropriate mathematical models to interpret the distribution of tracers such as ^{14}C and ^{3}H. Radioactive tracers were preferred because of high detection sensitivity, but these methods are limited by practical constraints, particularly for studies in human subjects. Perhaps less appreciated is the fact that the information yield from radiotracer experiments is inherently quite poor compared to the complexity of metabolism in vivo. For these reasons, the field has moved to the use of stable isotopes, particularly ^{13}C, with detection by mass spectrometry and NMR spectroscopy. Both technologies provide information about the labeling patterns in product molecules, which are inherently difficult or impossible to determine by radiotracer methods. If sample mass is adequate and the tissue can be conveniently biopsied, then analysis by either ^{13}C NMR or mass spectrometry can be considered. Both techniques offer valuable, quantitative insights into intermediary metabolism, an approach, which has recently proven valuable in cancer studies [3–7]. Mass spectrometry is more sensitive than NMR and can be done on smaller samples, while ^{13}C NMR is less sensitive and requires more sample but offers higher information yield.

The requirement of obtaining a tissue biopsy is a critical limitation, so there is great interest in obtaining truly noninvasively metabolic data from a tracer experiment. The advent of hyperpolarization (HP) technologies, described in detail elsewhere, enables real-time monitoring of metabolism of ^{13}C-enriched substrates in vivo, at least through a few enzyme-catalyzed steps. It is less comprehensive than steady-state isotopomer methods but as technical improvements come, it is likely

that noninvasive imaging with hyperpolarized ^{13}C coupled with metabolomics and mathematical analysis of metabolic pathways will enable fundamentally new concepts in disease pathophysiology. In this chapter, we summarize how HP ^{13}C has provided new insights into four important metabolic pathways and suggest possible further advances and limitations of the technique.

8.2 Pyruvate Dehydrogenase and the Krebs Cycle

Pyruvate dehydrogenase (PDH) catalyzes the conversion of pyruvate to acetyl-CoA and CO_2. PDH is a multienzyme complex located on the inner surface of the inner mitochondrial membrane. Flux through PDH is sensitive to mass-action and is regulated by both phosphorylation–dephosphorylation and the allosteric regulators, nicotinamide adenine dinucleotide hydrogen (NADH), and acetyl-CoA. The regulatory and phosphorylation sites are well established but the activity of the enzyme in vivo is not always known or easily predicted. [1-^{13}C]pyruvate is widely used in hyperpolarized ^{13}C studies, and it is generally assumed that the appearance of HP-bicarbonate reflects PDH activity and may provide an index of mitochondrial integrity. In highly oxidative tissues such as the heart, this may be true but two important factors should be considered when interpreting HP-bicarbonate production from [1-^{13}C]pyruvate.

The first issue is that PDH flux is very sensitive to competing substrates. Even in an isolated perfused heart where available substrates can be precisely controlled, the heart is still able to oxidize stored glycogen and triglycerides. In vivo, the heart is exposed to complex mixtures of short-, medium-, and long-chain fatty acids, glucose, lactate, and other oxidizable compounds that may vary widely in concentration and directly or indirectly influence PDH activity. The biochemical environment of PDH is difficult to monitor in vivo. Moreno et al. [8] demonstrated that the generation of HP-bicarbonate after exposure to HP-[1-^{13}C]pyruvate is very sensitive to competing substrates and that pyruvate polarization is altered by weak binding to albumin. In the presence of physiological levels of pyruvate (0.12 mM), lactate (1.2 mM), glucose (5 mM), ketones (0.17 mM), and fatty acids (0.4 mM), fatty acids and ketones overwhelmingly supply the majority of acetyl-CoA to the TCA cycle. However, with the addition of a bolus of pyruvate (3 mM to mimic HP conditions), pyruvate then provides ~80% of acetyl-CoA, while the contributions of ketones and fatty acids are reduced to near zero (Fig. 8.1). Under metabolic conditions mimicking a fast, meaning higher concentrations of ketones and fatty acids, HP-[^{13}C]bicarbonate production was much reduced. This indicates that the amount of HP-bicarbonate formed in an HP experiment will depend upon (1) dietary state and (2) the amount of HP-pyruvate reaching the tissue. Thus, under certain metabolic conditions, PDH could be fully active (dephosphorylated) even though production of HP-bicarbonate is relatively low because other substrates contribute more to the pool of acetyl-CoA entering the TCA cycle than HP-pyruvate. This means that it is possible to have a condition where the signal of HP [^{13}C]bicarbonate

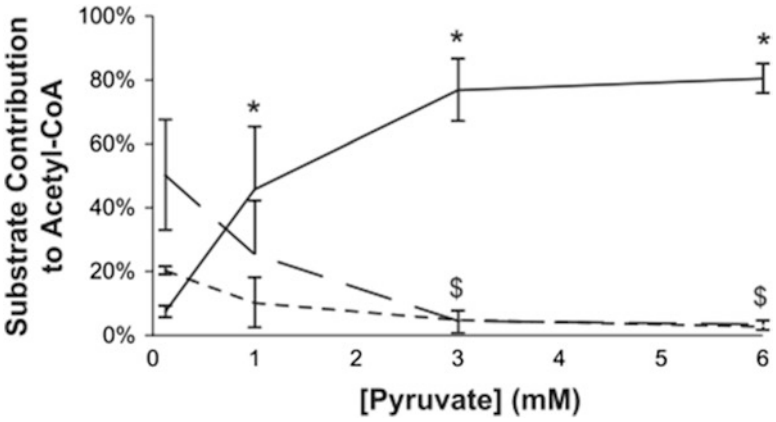

Fig. 8.1 Influence of [pyruvate] on sources of acetyl-CoA and flux through pyruvate dehydrogenase under fed conditions. Isolated hearts were supplied with a physiological mixture of fatty acids, ketones, and other substrates designed to replicate concentrations under fed, resting conditions. The relative rates of oxidation of ketones (dotted line), long-chain fatty acids (broken line), or pyruvate (solid line) are shown as a function of the [pyruvate]. At 3 mM pyruvate, oxidation of competing substrates is largely suppressed. Reproduced with permission from [8]. [APS statement: "Authors may republish parts of their final-published work (e.g., figures, tables), without charge and without requesting permission, provided that full citation of the source is given in the new work"]

approaches zero even when the activity of PDH is fully functional. It has also been shown that low concentrations of added propionate restore PDH flux even when the concentration of competing substrates is significant [9]. Thus, the interplay among normal regulation of PDH, physiological state of the animal or patient, and delivery must play an important role in a proper interpretation of an HP experiment.

A second important factor is the alternative pathway for HP [1-^{13}C]pyruvate to enter the TCA cycle via pyruvate carboxylase (PC) to form HP-[1-^{13}C]oxaloacetate which would also produce HP-bicarbonate after three or more forward steps in the TCA cycle (OAA → citrate → isocitrate → α-KG). The entry of pyruvate into the TCA cycle via PC, the dominant anaplerotic reaction in heart, is known to be small compared to forward flux through the TCA cycle (y_{pc} ~ 3–5% of TCA cycle flux) [10–13] so the production of HP-bicarbonate via this pathway should be relatively small. However, under metabolic conditions where fatty acids and ketones dominate production of acetyl-CoA, any production of HP-bicarbonate via entry of HP-pyruvate into the cycle via PC could be misinterpreted as reflecting flux through PDH.

Notwithstanding these potential limitations, the production of HP-bicarbonate from HP-[1-^{13}C]pyruvate has been reported to reflect PDH activity in cardiac tissue both in perfused hearts [14] and in vivo [15]. In isolated hearts, the addition of octanoate to compete with pyruvate for production of acetyl-CoA increased production of HP-lactate and reduced HP-bicarbonate production to near zero [14]. Nonpolarized ^{13}C isotopomer studies were used to verify that PDH flux was indeed

lower in the presence of octanoate while TCA cycle flux was unchanged. Thus, in a simple isolated perfused heart preparation where substrate availability is easily controlled, the production of HP-bicarbonate does appear to accurately reflect PDH activity. One might anticipate this may not be true in the in vivo myocardium because substrate availability (fed versus fasted) and pyruvate delivery could be added variables. Nonetheless, in rat hearts in vivo, Schroeder et al. [15] observed less production of HP-bicarbonate from HP-[1-^{13}C]pyruvate in both diabetic and 24 h starved rats compared to controls and ascribed these differences to reduced flux through PDH due to competition from higher plasma levels of fatty acids and ketone bodies. These physiological conditions also promote the phosphorylation of PDH via PDH kinase, which reduces the activity of PDH, consistent with their observations. Nevertheless, this study illustrates a common problem when faced with the interpretation of metabolic imaging studies based only on HP data. In this case, the question is, if less HP-bicarbonate is produced, does this reflect lower PDH activity or simply more competition from fatty acids, and ketone bodies for the production of acetyl-CoA? This question cannot be answered without additional supporting information.

Given that PDH flux is likely a good biomarker of intact mitochondria, there is a great deal of clinical interest in developing HP-[1-^{13}C]pyruvate to assess common heart diseases such as ischemia [16] or heart failure or to detect responses to drug interventions. Merritt et al. [17] evaluated the utility of HP [1-^{13}C]pyruvate to detect changes in PDH activity early vs. late after reperfusion of ischemic heart tissue, and compared the HP ^{13}C results with conventional ^{31}P NMR spectroscopic measures of PCr (phosphocreatine) and adenosine triphosphate (ATP) levels. Interestingly after brief ischemia followed by reperfusion, cardiac energetics and oxygen consumption were not sensitive to the earlier episode of ischemia, that is, these measures recovered quickly to preischemic levels. However, the appearance of HP [^{13}C]bicarbonate was impaired early after ischemia but recovered later, perhaps reflecting a highly reduced metabolic state immediately after the ischemic injury.

In a study designed to test whether a sudden increase in cardiac activity would stimulate flux of HP-[1-^{13}C]pyruvate through PDH to yield more HP-bicarbonate, isoproterenol was presented to perfused rat hearts ~30 s after each heart was exposed to HP-[1-^{13}C]pyruvate [18]. β-adrenergic stimulation resulted in a significant increase in heart rate from 290 to 420 beats/min but, surprisingly, no increase in the production of HP-bicarbonate from HP-[1-^{13}C]pyruvate. Those results are illustrated in Fig. 8.2. Instead, the signal of HP-lactate, which had already reached an apex in intensity ~20 s after the addition of HP-pyruvate, began to increase in intensity for a second time. This effect was later traced to the rapid breakdown of glycogen to form additional nonpolarized lactate, which was then available to exchange with the remaining HP-[1-^{13}C]pyruvate to generate a second lactate apex. This observation is interesting for two reasons. First, adrenergic stimulation of cardiac work did not increase flux through PDH as reported by the production of HP-bicarbonate. Instead, glycogen was rapidly converted to pyruvate and lactate to supply additional energy in the form of carbohydrates. Presumably, any HP-pyruvate remaining in the tissue after the addition of isoproterenol was quickly diluted by the

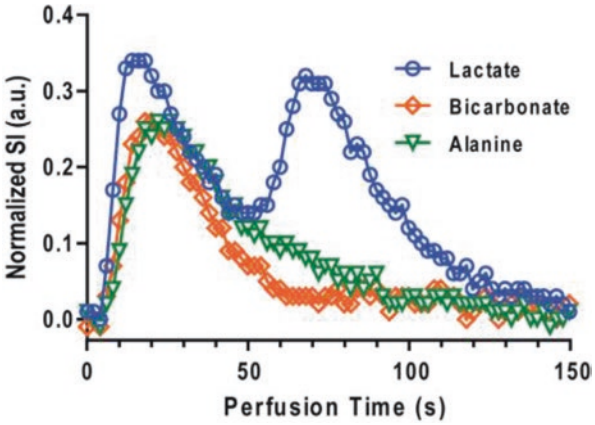

Fig. 8.2 Normalized ^{13}C resonance intensities versus time after the addition of HP-[1-^{13}C]pyruvate in isolated rat hearts. These data show the time-dependent signals of HP-lactate, alanine, and bicarbonate with additional isoproterenol at 30 s after the addition of HP [1-^{13}C]pyruvate. An elevated cardiac workload (as measured by heart rate and developed pressure) was achieved approximately 15 s after the addition of isoproterenol. Almost immediately thereafter, the signal intensity of HP-lactate which had begun to decay after reaching the first apex sharply increased in intensity and reached a second apex. Stimulation of cardiac function did not significantly alter the total HP bicarbonate signal. Reproduced with permission from [18]. [MRM statement: Authors—If you wish to reuse your own article (or an amended version of it) in a new publication of which you are the author, editor, or coeditor, prior permission is not required (with the usual acknowledgments)]

nonpolarized pyruvate generated from glycogenolysis and this resulted in no change in the appearance of HP-bicarbonate. This was further verified by isotopomer analysis of ^{13}C NMR spectra of tissue extracts. These results are consistent with the "glycogen shunt" hypothesis put forth by Shulman and Rothman [19] who suggested that the rapid breakdown of glycogen to lactate is absolutely required to buffer the short-term energy requirements of exercising muscle. This study further illustrates that the production of HP-bicarbonate from HP-[1-^{13}C]pyruvate is not necessarily an accurate biomarker of PDH flux.

Schroeder et al. [20] paced porcine hearts at a high rate over a period of several weeks to induce cardiomyopathy and periodically collected ^{31}P NMR spectra to monitor high-energy phosphates and ^{13}C NMR spectra after injection of either HP-[1-^{13}C]pyruvate or HP-[2-^{13}C]pyruvate to monitor downstream metabolic products (see Fig. 8.3). Unlike the use of [1-^{13}C]pyruvate where TCA cycle flux is assumed proportional to bicarbonate appearance (assuming appropriate control of competing substrates) [2-^{13}C]pyruvate is metabolized to [1-^{13}C]acetyl-CoA and eventually [5-^{13}C]glutamate, thereby directly interrogating the first span of the TCA cycle [21]. In this cardiomyopathy model, the myocardial PCr/ATP ratio progressively dropped throughout the pacing protocol from 2.3 ± 0.2 at baseline to 1.7 ± 0.1 at early pacing, and 1.3 ± 0.2 at moderate subclinical dysfunction. The amount of HP-[5-^{13}C]glutamate produced from HP-[2-^{13}C]pyruvate, considered an index of combined PDH activity and TCA cycle flux, also decreased in parallel with loss of

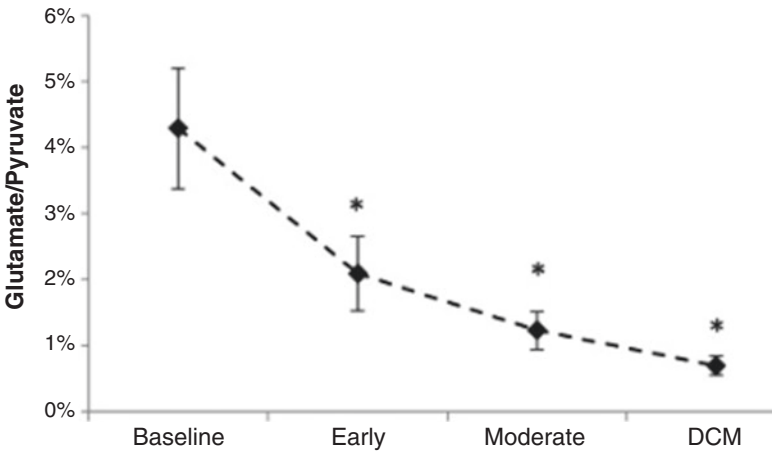

Fig. 8.3 Hyperpolarized ^{13}C magnetic resonance spectroscopy (MRS) showing altered [5-^{13}C]glutamate production during the development of dilated cardiomyopathy. Congestive heart failure was induced by long-term rapid pacing. Metabolism of HP-[2-^{13}C]pyruvate was repeatedly examined. Under these conditions, HP-[2-^{13}C]pyruvate is metabolized to HP-[5-^{13}C] α-ketoglutarate in the first span of the TCA cycle and subsequently to HP-[5-^{13}C]glutamate. The [5-^{13}C]glutamate/[2-^{13}C]pyruvate ratio is shown, measured for all pigs during development of heart failure. Reproduced with permission from [20]. [Permission granted from Eur. J. Heart Failure through RightsLink Copyright Clearance Center (https://s100.copyright.com/AppDispatchServlet)]

heart function while production of HP-bicarbonate remained equal to baseline levels over a much longer period, finally dropping at the end point of dilated cardiomyopathy. Although there may other interpretations of these data, this exciting study demonstrated for the first time that metabolic changes can be detected by HP ^{13}C metabolic imaging long before heart function actually deteriorates to a point where it is easily detected using standard clinical measures of left ventricular function. If such studies could be collected in the human myocardium well before irreversible heart failure sets in, then the administration of drugs or some other metabolic intervention could potentially save human lives.

The first hyperpolarized ^{13}C metabolic imaging study of the human heart using HP-[1-^{13}C]pyruvate was reported by Cunningham, et al. [22]. The metabolic images collected in that study, Fig. 8.4, show that HP-bicarbonate was mainly confined to the LV myocardium, whereas HP-[1-^{13}C]pyruvate appeared largely in the blood pool with little in the muscle itself while HP-[1-^{13}C]lactate produced via exchange with pyruvate appeared both within the chambers and in the myocardium. This nicely illustrates that information about myocardial metabolism and perhaps PDH flux can be obtained regionally within the tissue. One interesting feature of this study was that the amount of HP-bicarbonate produced from HP-[1-^{13}C]pyruvate appears to be considerably higher in human hearts compared to levels observed in rodent studies. This again illustrates that PDH flux is highly dependent upon dietary state, substrate delivery, and likely other yet to be determined factors. Most recently, hyperpolarized ^{13}C spectroscopy studies of the human heart were acquired in

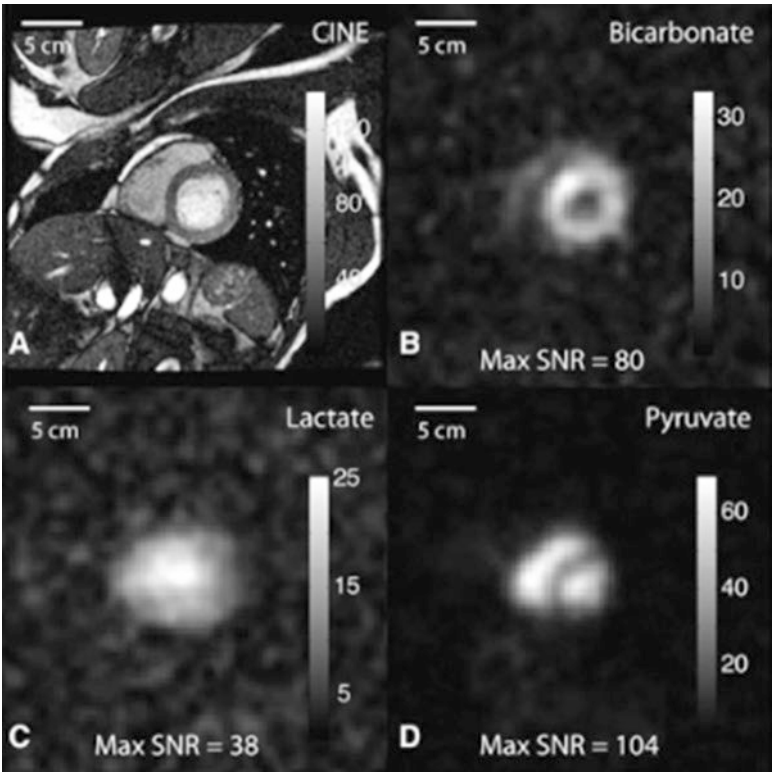

Fig. 8.4 Short axis anatomic and ^{13}C images from the heart of a healthy human subject. Panel (**a**) shows the anatomical image. Panel (**b**) shows the HP-bicarbonate image with an intense signal in the left ventricular myocardium and much less, although detectable, signal from the right ventricular myocardium. Panel (**c**) shows the HP [1-^{13}C]lactate image which appears to contain signal from both the blood pool and myocardium. Panel (**d**) is the HP[1-^{13}C]pyruvate image with, as expected, signal confined largely to the left and right ventricular cavities. Reproduced with permission from [22]. [Permission requested from AHA journals on 2/5/2019]

patients with type 2 diabetes [23], finding that flux through PDH was reduced among patients with type 2 diabetes. The effects of a cardiotoxic cancer therapy, doxorubicin, was studied in women with breast cancer [24]. A small decrease in flux through PDH but not LDH was observed in association with chemotherapy. In both studies, reduced PDH flux may be an indicator of subtle mitochondrial injury but again competition from other substrates should be considered.

The potential clinical significance of understanding PDH flux in the heart and other highly oxidative tissues is evident. Cancers are commonly thought to rely only on glycolysis for energy production (the Warburg phenomenon) but it has become clear that the TCA cycle may contribute significantly as well [5, 25, 26]. In isolated cancer cells [27] metabolism of HP-[1-^{13}C]pyruvate to HP bicarbonate was readily observed, but HP bicarbonate production in cancers in vivo is not commonly observed.

8.3 Pyruvate Carboxylase and Gluconeogenesis

Pyruvate carboxylase (PC) catalyzes the conversion of pyruvate to the 4-carbon TCA cycle intermediate, oxaloacetate. In some tissues, the dominant pathway for HP-[1-^{13}C]pyruvate could be the production of HP-[1-^{13}C]oxaloacetate rather than flux through PDH. PC is ubiquitous in virtually all tissues and is highly regulated. It requires biotin and one equivalent of ATP for activation of CO_2, and its activity is regulated by mitochondrial levels of acetyl-CoA:

$$\text{Pyruvate} + \text{HCO}_3^- + \text{ATP} \rightarrow \text{Oxaloacetate} + \text{ADP} + \text{Pi}.$$

PC is a critical anaplerotic reaction in the liver because it provides oxaloacetate in the first step of gluconeogenesis, in the brain where it is essential for the biosynthesis of neurotransmitters in astroglia, and in other tissues for net production of TCA cycle intermediates. In liver tissues where anaplerotic flux can be four- to sevenfold higher than TCA cycle flux [28, 29], drawing metabolic conclusions solely on the basis of HP-bicarbonate produced from HP-[1-^{13}C]pyruvate is tenuous. In this case (see Fig. 8.5), production of HP-bicarbonate could arise from flux through PDH (single step), carboxylation of HP-[1-^{13}C]pyruvate via PC followed by (a) forward flux in the TCA cycle (three steps) or (b) backward scrambling of 4-carbon intermediates followed by decarboxylation via PEPCK or the malic enzyme (at least three steps). Thus, it is not surprising to find little consensus in the literature as to which pathway dominates in producing $^{14}CO_2$ from [1-^{14}C]pyruvate. Some models of hepatic metabolism neglect flux through PDH entirely [30] or conclude that flux through PDH is small and even zero under some experimental conditions [31]. Others [32] assign the appearance of labeled bicarbonate only to flux through PDH.

In an early HP study of metabolism in isolated, perfused mouse livers, signals from HP-[1-^{13}C]malate and HP-[1-^{13}C]aspartate were evident within seconds after HP-[1-^{13}C]pyruvate was introduced into the perfusate [29, 33]. This provided direct evidence for the flux of HP-[1-^{13}C]pyruvate through PC as illustrated in Fig. 8.6. In addition to those signals, HP-bicarbonate was also observed. So this invoked the obvious question, does this bicarbonate reflect flux through PDH, the TCA cycle, or PEPCK? In an attempt to answer this question, mice lacking liver PEPCK were also examined, and in those livers, little HP-bicarbonate was detected. This suggested that the HP-bicarbonate seen in control mice might largely reflect flux of TCA cycle intermediates through PEPCK, an exciting result that, if true, suggests the bicarbonate signal could possibly be used as an index of gluconeogenesis. However, additional nonpolarized ^{13}C experiments using [1,2,3-$^{13}C_3$]pyruvate showed that pyruvate contributed ~7% of all acetyl-CoA in this preparation so clearly some HP-bicarbonate reflects PDH activity.

In the first in vivo liver study [34], the flux of HP-[1-^{13}C]pyruvate into TCA cycle intermediates via PC was also evident by the appearance of HP-[1-^{13}C]malate and HP-[1-^{13}C]aspartate resonances in the spectra. The kinetic rates of appearance of

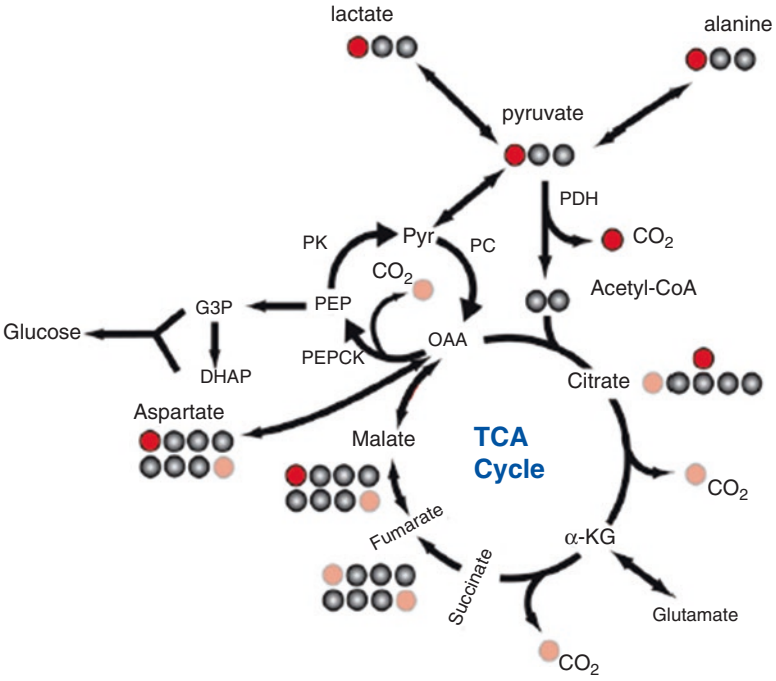

Fig. 8.5 Schematic of carbon flow in the liver originating from [1-^{13}C]pyruvate. The introduction of [1-^{13}C]pyruvate leads to labeling at the C1 of lactate and alanine (red circles). If PDH flux is present, CO_2 can also be labeled. If pyruvate carboxylase flux is significant, the label can appear at the C1 of malate. If the label is symmetrically distributed by the exchange between malate and fumarate, then it can also appear at the four positions of various metabolites (red, semitransparent circles). CO_2 can be eliminated by the action of either PEPCK on the C4 position of oxaloacetate or by enzymatic reactions in the forward span of the TCA cycle. Labeling of the CO_2 in these cases depends upon the level of symmetrization achieved by the malate to fumarate exchange. Reproduced with permission from [29]. [PNAS copyright: Anyone may, without requesting permission, use original figures or tables published in PNAS for noncommercial and educational use (i.e., in a review article, in a book that is not for sale), provided that the full journal reference is cited]

those signals ($k_{\text{pyr}\rightarrow\text{mal}}$ and $k_{\text{pyr}\rightarrow\text{asp}}$), presumably imaging biomarkers of PC flux, were higher in the liver of mice fed a high-fat diet. This correlated well with increased PC activity directly measured in tissue homogenate. This exciting study demonstrated for the first time that HP metabolic imaging could directly measure enzyme fluxes specific to liver in a type 2 model of diabetes. Nonetheless, the fact that little HP-bicarbonate was observed in these livers begs the question, why does one not detect upstream gluconeogenic products from these labeled TCA cycle intermediates? In principle, a relatively large amount of HP-bicarbonate should have been generated from these HP-intermediates, yet only a small HP-bicarbonate signal was observed. In this case, the appearance of HP-bicarbonate was ascribed entirely to flux through PDH without further direct experimental verification.

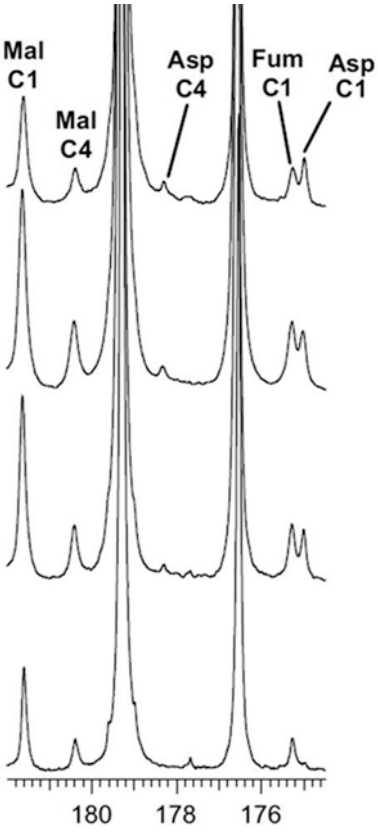

Fig. 8.6 ^{13}C NMR spectra during metabolism of hyperpolarized [2-^{13}C]- and [1-^{13}C]pyruvate. Signals of [1-^{13}C]lactate, [1-^{13}C]alanine and [1-^{13}C]pyruvate hydrate, [5-^{13}C]glutamate, [1-^{13}C]malate, [4-^{13}C]malate, [1-^{13}C]aspartate, [4-^{13}C]aspartate, and [1 or 4-^{13}C]fumarate were observed. Each panel represents livers perfused with different nonpolarized substrates prior to exposure to HP-pyruvate: (**a**) (1.5 mM) lactate and (0.15 mM) pyruvate; (**b**) (0.2 mM) octanoate; (**c**) (1.5 mM) lactate, (0.15 mM) pyruvate and (0.2 mM) octanoate; (**d**) (4 mM) pyruvate and (0.2 mM) octanoate. Reproduced with permission from Fig. 8.5 in ref. [33]. [Permission granted from Metabolomics through RightsLink Copyright Clearance Center (https://s100.copyright.com/AppDispatchServlet)]

In a second in vivo liver study, HP-bicarbonate was produced from HP-[1-^{13}C]pyruvate in the liver of fed rats but not in 21 h fasted rats [35]. In separate bench infusion studies in fed versus fasted animals, nonpolarized [2,3-$^{13}C_2$]pyruvate was used under identical conditions (bolus injection of 2.5 mL of 80 mM pyruvate) to validate and interpret the HP results. High-resolution ^{13}C NMR spectra of those liver extracts are shown in Fig. 8.7. The large doublet (labeled D45) in the glutamate C4 resonance of the liver extract from the fed animal shows that PDH is active (Fig. 8.7b). The very small D45 resonance in the spectrum of the fasted animal shows that PDH is relatively inactive under these feeding conditions. This is entirely

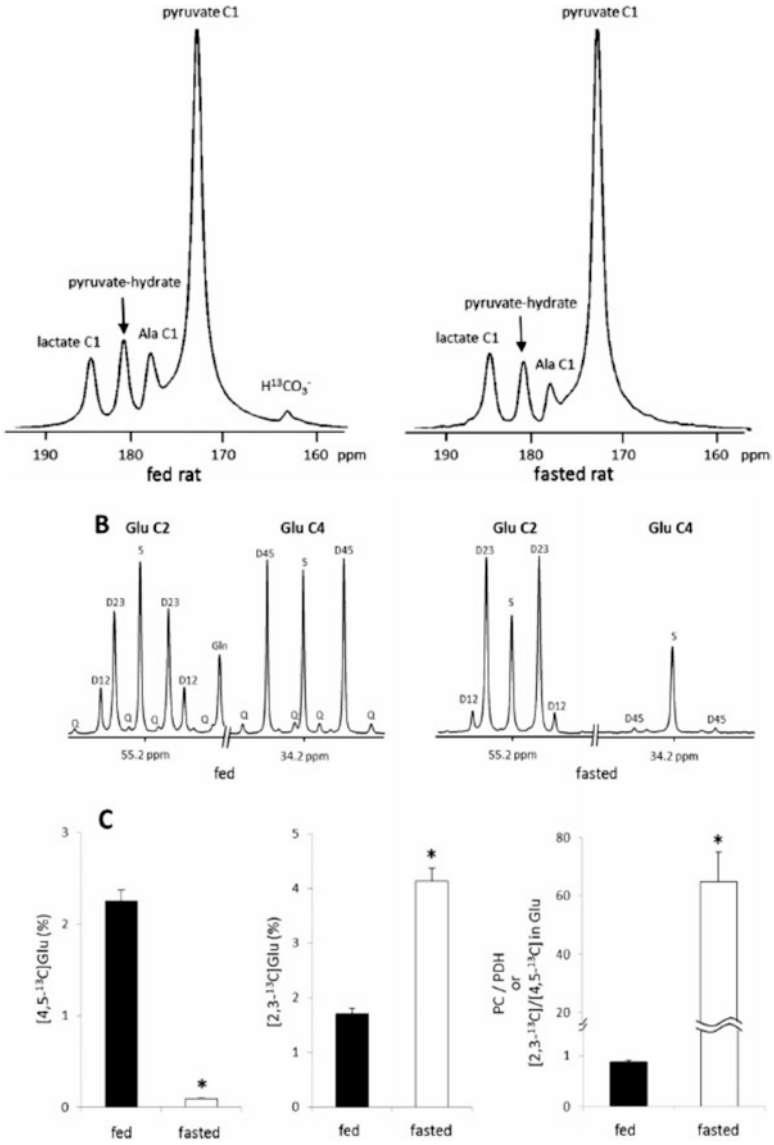

Fig. 8.7 Effect of nutritional state on integrated metabolic analysis of pyruvate carboxylation by conventional and hyperpolarized ^{13}C NMR. The upper panel shows ^{13}C NMR spectra of rat liver in vivo after intravenous injection of HP [1-^{13}C]pyruvate. Livers of both fed (left) and fasted (right) rats show HP signals from [1-^{13}C]lactate, [1-^{13}C]alanine, [1-^{13}C]pyruvate, and the hydrate of [1-^{13}C]pyruvate, but only livers of fed animals show the signal from HP [^{13}C]bicarbonate. The middle and bottom panels show results from conventional ^{13}C NMR isotopomer analysis after injection of [2,3-$^{13}C_2$]pyruvate and extraction at approximately the same time as the HP data. The entry of [2,3-$^{13}C_2$]pyruvate to the TCA cycle through PDH yields [4,5-^{13}C]glutamate while the entry through PC produces [2,3-$^{13}C_2$]glutamate after the condensation of [2,3$^{13}C_2$]oxaloacetate and acetyl-CoA followed by the forward turn through the TCA cycle. In ^{13}C NMR spectra of C2

consistent with the appearance of HP-bicarbonate in the liver of the fed animal and the absence of HP-bicarbonate in the liver from the fasted animal. Similarly, if [2,3-$^{13}C_2$]pyruvate enters the TCA cycle via PC to yield [2,3-$^{13}C_2$]oxaloacetate, then these labeled carbons would appear as D23 in the C2 resonance of glutamate. In the spectrum from the fed animal, the D23 is present but smaller than the C2 singlet while in the spectrum of the fasted animal, the D23 is larger than the C2 singlet. This directly shows that anaplerosis via PC is higher in the liver of fasted animals than in the liver from fed animals. Finally, the left bar graph in Fig. 8.7c shows that the relative PC/PDH flux ratio in the fasted animals is much higher than in fed animals, consistent with higher glucose production (GNG = gluconeogenesis) in the fasted state. Thus, the two in vivo liver HP studies report essentially the same thing: in mice fed a high-fat diet, the flux of HP-[1-^{13}C]pyruvate through PC is stimulated versus controls. In fasted rats where liver GNG is known to be high, PC flux as reported by ^{13}C isotopomer analysis is greatly stimulated overfed animals. Yet neither model provided evidence for the production of HP-bicarbonate from HP-oxaloacetate via PEPCK, the first committed step in GNG. This is rather unexpected given that HP-malate, HP-aspartate, and HP-glutamate have all been detected in various tissues. Other studies in isolated livers where a detailed analysis of pathway fluxes based on direct measurements of oxygen consumption and ketone production also concluded that bicarbonate production did not correlate well with pyruvate carboxylation [33] in spite of high flux through PEPCK. Might there be a biological reason for the loss of spin polarization at the level of PEPCK?

One can only speculate at this point but a potential source for depolarization can be gleaned from the crystal structure of PEPCK [36, 37]. PEPCK is a GTP-dependent enzyme that catalyzes decarboxylation and concomitant phosphorylation of oxaloacetate to form PEP:

$$\text{Oxaloacetate} + \text{GTP} \rightarrow \text{CO}_2 + \text{GDP} + \text{PEP}\left(\text{Phosphoenolpyruvate}\right).$$

The rat liver cytosolic form of the enzyme contains a paramagnetic Mn^{2+} ion in the active site that binds to an oxygen atom on the C1 carboxyl group plus the carbonyl oxygen atom on C2 [37]. Binding of Mn^{2+} to the C2 carbonyl oxygen stabilizes the enol form of OAA, which weakens the C3–C4 bond and promotes release of the C4 carboxyl group as CO_2, as illustrated in Fig. 8.8. Simultaneous with the release of CO_2, the nucleophilic enol oxygen on C2 attacks the γ-phosphate of GTP to form PEP and GDP. A divalent Mg^{2+} bound to the α- and β-phosphates of GTP

Fig. 8.7 (continued) (~55.2 ppm) and C4 (~34.2 ppm) regions of glutamate isolated from liver, the signal from [4,5-$^{13}C_2$]glutamate is strong in fed animals, but negligible in fasted rats. The signal from [2,3-$^{13}C_2$]glutamate is easily detected in fed animals and very strong in fasted animals. The ratio of [2,3-$^{13}C_2$]/[4,5-$^{13}C_2$] in glutamate, reflecting the ratio of PC/PDH, was dramatically higher in fasted rats compared with fed rats. Reproduced with permission from [35]. [NMR in Biomedicine statement: Authors—If you wish to reuse your own article (or an amended version of it) in a new publication of which you are the author, editor, or coeditor, prior permission is not required (with the usual acknowledgments)]

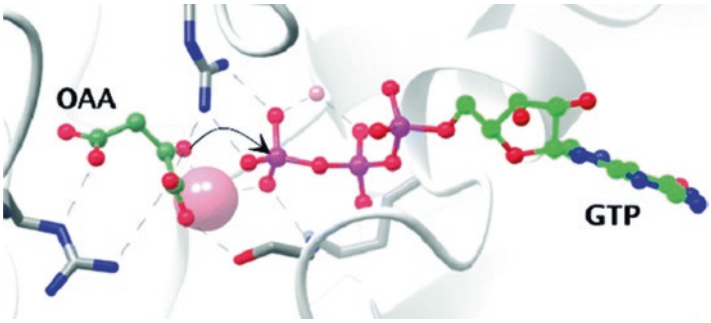

Fig. 8.8 Structure of the Mn^{2+}-OAA-GTP complex in the active site of PEPCK. The large pink sphere represents Mn^{2+} coordinated to both the C1 and C2 oxygen atoms of OAA and the γ-phosphate of GTP. The other active site ligands coordinated to the Mn^{2+} ions were omitted for clarity. Reproduced with permission from [37]. [Permission granted from Biochemistry through RightsLink Copyright Clearance Center (https://s100.copyright.com/AppDispatchServlet)]

sits nearby the Mn^{2+} and aids in the release of the γ-phosphate. Given that Mn^{2+} has five unpaired electrons and is quite efficient at relaxing nearby NMR nuclei (r^{-6} dependence), it is reasonable to assume that all highly polarized OAA ^{13}C atoms could be rapidly relaxed by the paramagnetic Mn^{2+} ion when OAA binds in the active site of PEPCK. This may be the reason why we have not been able to conclusively assign production of HP-bicarbonate to flux through PEPCK even under conditions when highly polarized 4-carbon TCA cycle intermediates can be detected and gluconeogenesis is active.

8.4 Glycolysis

Given the importance of glucose as an energy source and a source of carbons for many biosynthetic processes, the possibility of imaging intermediates along those many pathways using HP ^{13}C probes is very appealing. Unfortunately, carbohydrates are not great candidates for HP ^{13}C imaging because most carbons have at least one directly attached proton and this reduces the T_1 of a directly bonded ^{13}C atom via dipolar interactions. Those directly bonded protons can be substituted with deuterium to lengthen the carbon T_1 values [38] but even with this modification, the T_1s are rather short (~10–12 s). Nevertheless, [U-$^{2}H_7$, U-$^{13}C_6$]glucose has been polarized and investigated in suspensions of *Escherichia coli* [39], yeast [40–42], and breast cancer cells [43] and in an in vivo lymphoma mouse model [44]. In *E. coli*, resonances characteristic of gluconate-6-phosphate (6-PGA), fructose-1,6-bisphosphate (FBP), dihydroxyacetone phosphate (DHAP), pyruvate, acetyl-CoA, lactate, alanine, acetate, formate, CO_2, HCO_3^-, ribulose-5P, and ethanol where all observed within a few seconds after delivery of HP-[U-$^{2}H_7$, U-$^{13}C_6$]glucose to a cell suspension. This demonstrates that multiple pathway intermediates can be detected

in living cells, and the kinetics of the appearance of HP-carbons in those intermediates can provide few new insights into metabolic control. Nonetheless, a comparison of labeled intermediates in exponentially growing cells versus stationary phase cells showed that more glucose is converted to δ-6-phosphogluconolactone (five-fold) in the former, consistent with greater flux through the oxidative branch of the pentose phosphate pathway during the cell growth phase [39]. Similarly, in fermenting yeast cells, FBP, 6-phosphogluconate, and pyruvate along with the catabolic end products, ethanol, and CO_2, were rapidly produced from HP-[U-$^{2}H_7$, U-$^{13}C_6$]glucose in a real-time DNP-NMR assay. The appearance of HP-pyruvate and HP-ethanol versus lack of appearance of HP-acetaldehyde was ascribed to the well-known rate-limiting pyruvate decarboxylase reaction [45] and rapid conversion of acetaldehyde to ethanol.

Although HP studies in isolated cells have not revealed anything substantially new about metabolism or metabolic flux compared to more traditional tracer experiments, they do offer the huge advantage of rapid detection so that physiological responses to any specific metabolic intervention can be assayed quickly, an important advantage in biotechnical optimization of cellular networks [39]. HP-[U-$^{2}H_7$, U-$^{13}C_6$]glucose has also been exposed to T47D breast cancer cells [43] and, in this case, fewer intermediates (DHAP, 3PG, lactate) were directly visible by ^{13}C NMR in comparison to those detected in yeast and *E. coli*. Nevertheless, given that the chemical shift of most glycolytic intermediates is well established, a unique radio-frequency pulse saturation method was used to indirectly monitor relative flux from several "invisible" metabolites to lactate [43]. It was shown that the appearance of HP-lactate from HP-glucose followed Michaelis-Menten-like kinetics with a $K_m = 3.5 \pm 1.5$ mM and $V_{max} = 34 \pm 4$ fmol/cell/min [43], values completely consistent with earlier reported constants. One question that arises whenever perdeuterated glucose is used for polarization studies is the possible impact of a deuterium kinetic isotope effect on measured kinetic rate constants. Funk et al. [46] recently demonstrated using isotopomer methods that the rate of conversion of [U-$^{13}C_6$]glucose to lactate versus [U-$^{13}C_6$,U-$^{2}H_7$]glucose to lactate does not differ in isolated perfused rat hearts so this suggests that kinetic constants measured by the appearance of HP-lactate from HP-deuterated glucose should accurately reflect glycolysis.

HP-[U-$^{2}H_7$, U-$^{13}C_6$]glucose has also been used to image glycolysis in an in vivo lymphoma EL4 tumor model [44]. This was the first report of the detection of HP-lactate, the end-product of glycolysis, from HP-glucose in vivo. Unlike in cell suspensions where a sample of highly polarized [U-$^{2}H_7$, U-$^{13}C_6$]glucose can be mixed quickly with cells already suspended in an NMR tube in a magnet, in vivo detection requires blood circulation and cell uptake of HP-[U-$^{2}H_7$, U-$^{13}C_6$]glucose before entering glycolysis so this first report stimulated great excitement among the metabolic imaging community. Indeed, low levels of DHAP, 6-phosphogluconate (6PG), and bicarbonate (HCO_3^-) were also detected in those tumors, but the signal from HP-lactate demonstrated for the first time that the entire glycolytic pathway can potentially be monitored in real time. Given the importance of the Warburg effect in tumors and the possibility of imaging the impact of cancer drugs on glycolysis, this was an important scientific observation. Unfortunately, other tumors

are much less glycolytic than the EL4 tumor so, unlike HP-pyruvate, HP-[U-$^{2}H_7$, U-$^{13}C_6$]glucose has yet to become a widely used probe in metabolic imaging.

In an attempt to further lengthen the T_1 of glucose, [U-$^{2}H_7$, 3,4-$^{13}C_2$]glucose was prepared and its relaxation properties compared with those of HP-[U-$^{2}H_7$, U-$^{13}C_6$]glucose [47]. The idea in creating [U-$^{2}H_7$, 3,4-$^{13}C_2$]glucose was to reduce the number of carbon–carbon spin–spin interactions within glucose such that when [U-$^{2}H_7$, 3,4-$^{13}C_2$]glucose undergoes glycolysis, it produces singly C1-labeled, largely nonprotonated glycolytic intermediates from [1-^{13}C]1,3-*bis*-P-glycerate to [1-^{13}C]lactate in the glycolytic pathway. Any HP-[1-^{13}C]lactate formed from HP-[U-$^{2}H_7$, 3,4-$^{13}C_2$]glucose would also appear as a singlet instead of a doublet and this would essentially improve *S*/*N* by an added factor of 2. Although the differences in carbon T_1s between the two labeled glucose molecules were small, the added advantage of having a singlet in [1-^{13}C]lactate did prove beneficial in that HP-lactate was clearly detected in the brain of a live mouse within about 10 s after tail vein delivery of HP-[U-$^{2}H_7$, 3,4-$^{13}C_2$]glucose [47]. Although this was once again a nice demonstration of the potential of HP ^{13}C for imaging the glycolytic pathway, the T_1s of glucose will likely limit applications to mouse models of cancer and perhaps traumatic brain injury. The prospects of translating this technology to humans seem remote at this point in technology development.

Given that some glycolytic intermediates contain nonprotonated carbons, other longer T_1 hyperpolarized probes of glycolysis have been investigated. Park et al. [48] polarized [1-^{13}C]glycerate and observed its biochemical conversion to [1-^{13}C]pyruvate and [1-^{13}C]lactate in vivo in rat liver. The T_1 of this probe (~60 s at 3 T) was sufficiently long for the molecule to be transported into hepatocytes via monocarboxylate transporters, phosphorylated to 3-phospho-[1-^{13}C]glycerate (3PG), and converted to the glycolytic end products, HP-[1-^{13}C]pyruvate and HP-[1-^{13}C]lactate with excellent signal-to-noise. Although small differences were observed in the amount of HP-[1-^{13}C]lactate formed in fed versus fasted animals, the most interesting observation of the study was that both HP-pyruvate and HP-lactate were directly detected, thereby offering possible use of this probe as an indicator of cytosolic redox state.

A second small molecule containing a nonprotonated carbon that has been considered as an HP probe of glycolysis is [2-^{13}C]dihydroxyacetone [49]. This neutral molecule also quickly enters hepatocytes, becomes phosphorylated, and enters the glycolytic pathway at the level of triosephosphate isomerase (TPI), slightly upstream of 3PG. Although the T_1 of this probe is about 50% shorter (~32 s at 9.4 T) than 3PG, the phosphorylated product, HP-[2-^{13}C]DHAP, showed many more detectable glycolytic intermediates in the liver, both downstream (glyceraldehyde-3-P, 3PG, PEP, pyruvate, lactate, and alanine) and upstream (glycerol-3-P, glucose-6-P, and glucose) of TPI. This indicates that HP-[2-^{13}C]dihydroxyacetone, unlike HP-[1-^{13}C]glycerate, provides a broader metabolic snapshot of both glycolysis and gluconeogenesis from triose to glucose. These probe differences suggest that there is an important point of regulation between these two entry points, perhaps at the level of glyceraldehyde-3-P dehydrogenase. A second feature of the [2-^{13}C]dihydroxyacetone study that was not evident in the [1-^{13}C]glycerate study was the detection of both

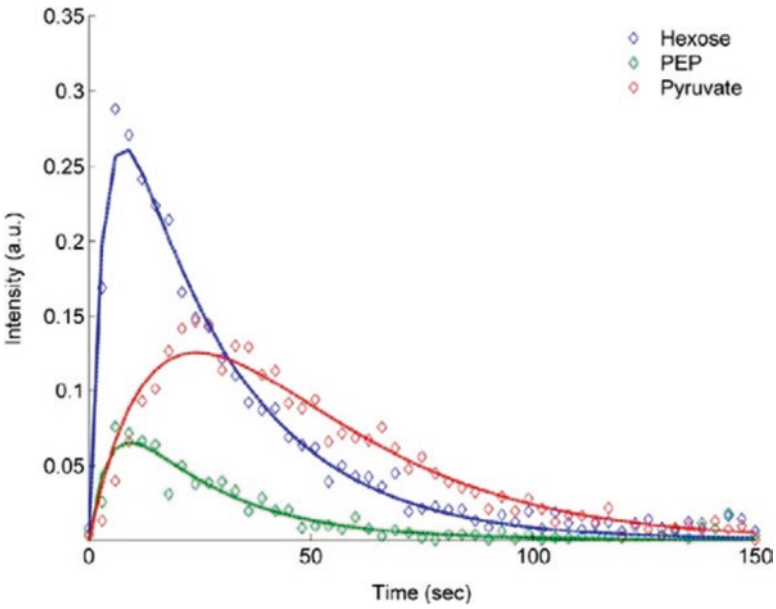

Fig. 8.9 Time course for hyperpolarized metabolites of dihydroxyacetone in the gluconeogenic state. Hexose denotes the sum of all the hexose resonances, while PEP and pyruvate refer only to the individual metabolites. Pyruvate kinase is the only enzyme of the glycolytic–gluconeogenic pathway that produces a delay in the kinetic curves. Units are arbitrary. Reproduced with permission from [49]. [JBC: Authors of manuscripts, submitted at any time, need not contact the journal to request permission to reuse their own material]

HP-PEP and HP-pyruvate when using [2-^{13}C]dihydroxyacetone. The kinetic curves (see Fig. 8.9) show a rather substantial delay in the appearance of HP-pyruvate compared to HP-PEP, which suggests that the activity of pyruvate kinase can be readily monitored using this most interesting new HP probe.

8.5 Pentose Phosphate Pathway

Reduced nicotinamide adenine dinucleotide phosphate (NADPH) plays a key role in metabolism in at least two respects. It is an essential cofactor in reductive biosynthetic pathways such as de novo lipogenesis from acetyl-CoA and is required for the regeneration of glutathione, a reaction catalyzed by glutathione reductase (GSSG → 2GSH) in response to oxidative stress. Two equivalents of NADPH are produced in the first two enzymes in the pentose phosphate pathway, glucose-6-phosphate dehydrogenase (G6PD) and 6-phosphogluconolactonase (6PGDH). The generation of NADPH might be particularly important for studies related to nutritional excess—very important in western societies—because the PPP is assumed to be essential for both de novo lipogenesis to store excess calories and glutathione reduction to

protect against oxidative stress with excess nutrition [50]. The PPP is upregulated in tissues with oxidative stress related to brain trauma and in cancer to provide ribose for nucleotide biosynthesis. However, very little is known about the activity of the PPP in the evolution of these diseases so noninvasive methods to monitor this pathway flux could have a substantial impact in future studies of human patients.

In the irreversible oxidative phase of the pentose phosphate pathway, glucose-6-phosphate is oxidized to glucono-δ-lactone-6-phosphate, which is hydrolyzed and decarboxylated to ribulose-5-phosphate plus CO_2. We recently reported that the production of hyperpolarized bicarbonate can be detected in isolated livers supplied with [1-^{13}C]-D-glucono-δ-lactone, a convenient water-soluble metabolite that is rapidly taken up by the liver [51]. In that study, HP[1-^{13}C]-D-glucono-δ-lactone was used as a probe to detect flux through the oxidative portion of the pentose phosphate pathway (PPP_{ox}). The appearance of HP $H^{13}CO_3^-$ within seconds after exposure of livers to HP[1-^{13}C]-D-glucono-δ-lactone (Fig. 8.10) demonstrated that this probe rapidly enters hepatocytes, becomes phosphorylated, and enters the PPP_{ox} pathway to produce HP-$H^{13}CO_3^-$ after three enzyme-catalyzed steps (6P-gluconolactonase, 6-phosphogluconate dehydrogenase, and carbonic anhydrase). Livers perfused with octanoate as their sole energy source show no change in the production of HP-$H^{13}CO_3^-$ after exposure to low levels of H_2O_2, while livers perfused with glucose and insulin showed a twofold increase in HP-$H^{13}CO_3^-$ after exposure to

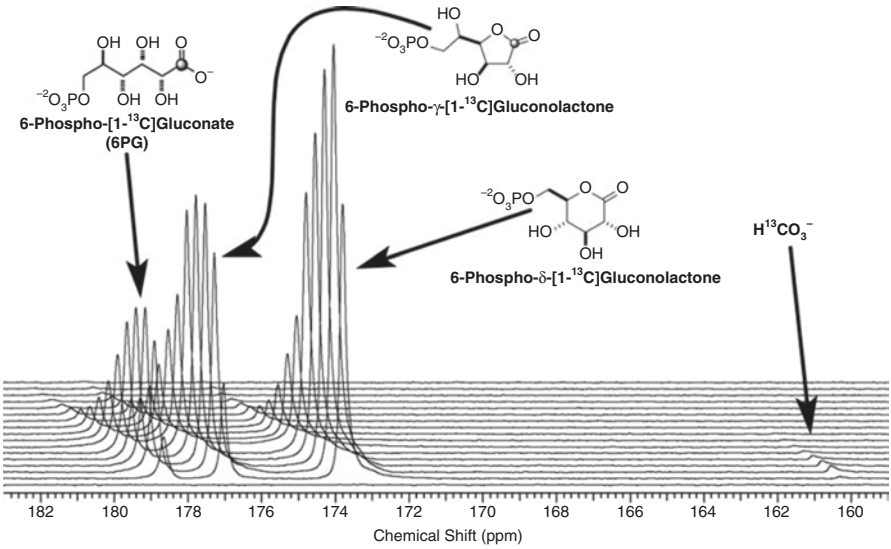

Fig. 8.10 A stacked plot of ^{13}C NMR spectra collected on an isolated mouse liver after the continuous addition of hyperpolarized [1-^{13}C]-D-glucono-δ-lactone. The ^{13}C spectra were collected every 5 s using a 66° pulse. Reproduced with permission from [51]. [NMR in Biomedicine statement: AUTHORS—If you wish to reuse your own article (or an amended version of it) in a new publication of which you are the author, editor, or coeditor, prior permission is not required (with the usual acknowledgments)]

peroxide. This indicates that flux through the PPP_{ox} is stimulated by H_2O_2 in livers perfused with glucose but not in livers perfused with octanoate alone. Subsequent perfusion of livers with nonpolarized [1,2-$^{13}C_2$]glucose followed by ^{1}H NMR analysis of lactate in the perfusate verified that flux through the PPP_{ox} is indeed low in healthy livers and modestly higher in peroxide-damaged livers. We conclude that hyperpolarized [1-^{13}C]-D-glucono-δ-lactone has the potential to serve as a metabolic imaging probe of this important biological pathway.

8.6 Quantitation: Proceed with Caution

In some respects, the use of hyperpolarized ^{13}C-enriched substrates such as pyruvate, acetate, lactate, α-ketoglutarate, and glutamine is conceptually quite similar to analogous radiotracer experiments. Compared to radiotracer exams, however, HP is distinctive in three respects. *First*, the mass of administered material is massively greater than the comparable radiotracer experiment. Although the exams appear to be well tolerated, investigators should consider that the mass of infused pyruvate or other substrates could have direct metabolic effects on the system. *Second*, the appearance of downstream metabolites will be sensitive to T_1 losses in upstream compartments. For example, the metabolism of HP-[1-^{13}C]pyruvate to HP-bicarbonate and acetyl-CoA occurs in the mitochondria matrix, which has very low water content. The immediate product, HP $^{13}CO_2$, must exit the matrix and react with water via carbonic anhydrase to generate HP-bicarbonate. It is difficult to know the T_1 of intramitochondrial $^{13}CO_2$, yet the T_1 must have an effect on the appearance of HP-bicarbonate. *Third*, the specifics of data acquisition will influence the observed kinetics. Every observe pulse depletes some magnetization so pulses on upstream metabolites such as pyruvate may influence the appearance of downstream metabolites such as bicarbonate. Each of these factors could influence the signal observed in an HP exam and the mathematical models developed for radiotracer kinetics will likely need appropriate modification.

8.7 Summary

Metabolism plays a central role in all body processes, and these processes are disrupted in virtually all of the high-impact diseases of western societies. Because of their complexity, probing these networks in vivo using radiotracers provides only limited insight. The use of ^{13}C as a tracer with detection by NMR is a far richer source of information about tracer distribution but the low sensitivity of ^{13}C for NMR detection excludes meaningful imaging of this nucleus in vivo. Hyperpolarization is an example of new applications of well-known physics that provides a method to probe metabolic events at the cellular, organ, and systemic level. Coupled with metabolomics tools and mathematical analysis of metabolic

pathways, new insights in physiopathology are likely. Although applications to biological systems are a relatively new field, hyperpolarization has enabled new insights in some fundamental metabolic pathways. MRI of hyperpolarized ^{13}C-enriched metabolites offers considerable potential as a rapid, noninvasive tool for detecting changes in metabolic fluxes in patients.

Acknowledgments The authors thank the NIH for grant support (P41-EB015908 and R37-HL034557) during the writing of this review.

Problems

1. Production of HP-bicarbonate from HP-[1-^{13}C]pyruvate in the myocardium is thought to reflect the tissue activity of pyruvate dehydrogenase (PDH). Since PDH is a large complex embedded in mitochondria, appearance of HP-bicarbonate might be a good index of mitochondrial integrity. Suppose you perform an HP experiment in vivo and observe very little production of HP-bicarbonate in the heart of an obese rat after injection of HP-[1-^{13}C]pyruvate.
   (a) Does this mean that mitochondria in the heart are defective? Why or why not?
   (b) Suggest a physiological manipulation one might do in vivo to test your conclusion.
2. In the liver, the anaplerotic flux of pyruvate into the TCA cycle via pyruvate carboxylase (PC) is reportedly three- to sixfold higher than the TCA cycle flux itself. Assuming an average of fivefold for a particular metabolic state, calculate the fraction of HP-bicarbonate that would be produced by the entry of HP-[1-^{13}C]pyruvate via PDH versus entry of HP-[1-^{13}C]pyruvate via PC followed by either forward flux through the TCA cycle or PEPCK. State your assumptions. Assume all HP-bicarbonate produced in these pathways is detectable by ^{13}C NMR.
3. Nonhyperpolarized [1,2-^{13}C]glucose has been used as a biomarker of the oxidative pentose phosphate pathway, PPP_{ox}, activity by analysis of the ^{13}C NMR spectrum of lactate produced from this starting material. Suggest an alternative ^{13}C-enriched derivative of glucose that could potentially be used as an HP probe of PPP_{ox} activity. Explain which HP signals one might detect and how these relate to PPP_{ox} activity.

References

1. Collins, R.R.J., Patel, K., Putnam, W.C., Kapur, P., Rakheja, D.: Oncometabolites: a new paradigm for oncology, metabolism, and the clinical laboratory. Clin. Chem. **63**, 1812–1820 (2017)
2. Yang, M., Soga, T., Pollard, P.J.: Oncometabolites: linking altered metabolism with cancer. J. Clin. Invest. **123**, 3652–3658 (2013)

3. Faubert, B., Li, K.Y., Cai, L., Hensley, C.T., Kim, J., Zacharias, L.G., Yang, C., Do, Q.N., Doucette, S., Burguete, D., et al.: Lactate metabolism in human lung tumors. Cell. **171**, 358–371 (2017) e359
4. Hensley, C.T., Faubert, B., Yuan, Q., Lev-Cohain, N., Jin, E., Kim, J., Jiang, L., Ko, B., Skelton, R., Loudat, L., et al.: Metabolic heterogeneity in human lung tumors. Cell. **164**, 681–694 (2016)
5. Maher, E.A., Marin-Valencia, I., Bachoo, R.M., Mashimo, T., Raisanen, J., Hatanpaa, K.J., Jindal, A., Jeffrey, F.M., Choi, C., Madden, C., et al.: Metabolism of [U-13 C]glucose in human brain tumors in vivo. NMR Biomed. **25**, 1234–1244 (2012)
6. Mashimo, T., Pichumani, K., Vemireddy, V., Hatanpaa, K.J., Singh, D.K., Sirasanagandla, S., Nannepaga, S., Piccirillo, S.G., Kovacs, Z., Foong, C., et al.: Acetate is a bioenergetic substrate for human glioblastoma and brain metastases. Cell. **159**, 1603–1614 (2014)
7. Sellers, K., Fox, M.P., Bousamra 2nd, M., Slone, S.P., Higashi, R.M., Miller, D.M., Wang, Y., Yan, J., Yuneva, M.O., Deshpande, R., et al.: Pyruvate carboxylase is critical for non-small-cell lung cancer proliferation. J. Clin. Invest. **125**, 687–698 (2015)
8. Moreno, K.X., Sabelhaus, S.M., Merritt, M.E., Sherry, A.D., Malloy, C.R.: Competition of pyruvate with physiological substrates for oxidation by the heart: implications for studies with hyperpolarized [1-13C]pyruvate. Am. J. Physiol. Heart Circ. Physiol. **298**, H1556–H1564 (2010)
9. Purmal, C., Kucejova, B., Sherry, A.D., Burgess, S.C., Malloy, C.R., Merritt, M.E.: Propionate stimulates pyruvate oxidation in the presence of acetate. Am. J. Physiol. Heart Circ. Physiol. **307**, H1134–H1141 (2014)
10. Jeffrey, F.M., Rajagopal, A., Malloy, C.R., Sherry, A.D.: 13C-NMR: a simple yet comprehensive method for analysis of intermediary metabolism. Trends Biochem. Sci. **16**, 5–10 (1991)
11. Malloy, C.R., Sherry, A.D., Jeffrey, F.M.: Carbon flux through citric acid cycle pathways in perfused heart by 13C NMR spectroscopy. FEBS Lett. **212**, 58–62 (1987)
12. Malloy, C.R., Sherry, A.D., Jeffrey, F.M.: Evaluation of carbon flux and substrate selection through alternate pathways involving the citric acid cycle of the heart by 13C NMR spectroscopy. J. Biol. Chem. **263**, 6964–6971 (1988)
13. Malloy, C.R., Sherry, A.D., Jeffrey, F.M.: Analysis of tricarboxylic acid cycle of the heart using 13C isotope isomers. Am. J. Phys. **259**, H987–H995 (1990)
14. Merritt, M.E., Harrison, C., Storey, C., Jeffrey, F.M., Sherry, A.D., Malloy, C.R.: Hyperpolarized 13C allows a direct measure of flux through a single enzyme-catalyzed step by NMR. Proc. Natl. Acad. Sci. U. S. A. **104**, 19773–19777 (2007)
15. Schroeder, M.A., Cochlin, L.E., Heather, L.C., Clarke, K., Radda, G.K., Tyler, D.J.: In vivo assessment of pyruvate dehydrogenase flux in the heart using hyperpolarized carbon-13 magnetic resonance. Proc. Natl. Acad. Sci. U. S. A. **105**, 12051–12056 (2008)
16. Golman, K., Petersson, J.S., Magnusson, P., Johansson, E., Akeson, P., Chai, C.M., Hansson, G., Mansson, S.: Cardiac metabolism measured noninvasively by hyperpolarized 13C MRI. Magn. Reson. Med. **59**, 1005–1013 (2008)
17. Merritt, M.E., Harrison, C., Storey, C., Sherry, A.D., Malloy, C.R.: Inhibition of carbohydrate oxidation during the first minute of reperfusion after brief ischemia: NMR detection of hyperpolarized 13CO2 and H13CO3. Magn. Reson. Med. **60**, 1029–1036 (2008)
18. Khemtong, C., Carpenter, N.R., Lumata, L.L., Merritt, M.E., Moreno, K.X., Kovacs, Z., Malloy, C.R., Sherry, A.D.: Hyperpolarized 13C NMR detects rapid drug-induced changes in cardiac metabolism. Magn. Reson. Med. **74**, 312–319 (2015)
19. Shulman, R.G., Rothman, D.L.: The "glycogen shunt" in exercising muscle: a role for glycogen in muscle energetics and fatigue. Proc. Natl. Acad. Sci. U. S. A. **98**, 457–461 (2001)
20. Schroeder, M.A., Lau, A.Z., Chen, A.P., Gu, Y., Nagendran, J., Barry, J., Hu, X., Dyck, J.R., Tyler, D.J., Clarke, K., et al.: Hyperpolarized (13)C magnetic resonance reveals early- and late-onset changes to in vivo pyruvate metabolism in the failing heart. Eur. J. Heart Fail. **15**, 130–140 (2013)
21. Schroeder, M.A., Atherton, H.J., Ball, D.R., Cole, M.A., Heather, L.C., Griffin, J.L., Clarke, K., Radda, G.K., Tyler, D.J.: Real-time assessment of Krebs cycle metabolism using hyperpolarized 13C magnetic resonance spectroscopy. FASEB J. **23**, 2529–2538 (2009)

22. Cunningham, C.H., Lau, J.Y., Chen, A.P., Geraghty, B.J., Perks, W.J., Roifman, I., Wright, G.A., Connelly, K.A.: Hyperpolarized 13C metabolic MRI of the human heart: initial experience. Circ. Res. **119**, 1177–1182 (2016)
23. Rider, O.J., Apps, A., Miller, J.J.J.J., Lau, J.Y.C., Lewis, A.J.M., Peterzan, M.A., Dodd, M.S., Lau, A.Z., Trumper, C., Gallagher, F.A., Grist, J.T., Brindle, K.M., Neubauer, S., Tyler, D.J.: Noninvasive In Vivo Assessment of Cardiac Metabolism in the Healthy and Diabetic Human Heart Using Hyperpolarized 13C MRI. Circ. Res. **126**, 725–736 (2020)
24. Park, J.M., Reed, G.D., Liticker, J., Putnam, W.C., Chandra, A., Yaros, K., Afzal, A., MacNamara, J.P., Raza, J., Hall, R.G., Baxter, J., Derner, K., Pena, S., Kallem, R.R., Subramanyan, I., Edpuganti, V., Harrison, C., Muthukumar, A., Lewis, C., Reddy, S., Unni, N., Klemow, D., Syed, S., Li, H.C., Cole, S.M., Froehlich, T., Ayers, C.R., de Lemos, J.A., Malloy, C.R., Haley, B., Zaha, V.G.: Effect of Doxorubicin on Myocardial Bicarbonate Production from Pyruvate Dehydrogenase in Women with Breast Cancer. Circ Res. 2020 Oct 14. https://doi.org/10.1161/CIRCRESAHA.120.317970. Epub ahead of print. PMID: 33054563
25. Marin-Valencia, I., Cho, S.K., Rakheja, D., Hatanpaa, K.J., Kapur, P., Mashimo, T., Jindal, A., Vemireddy, V., Good, L.B., Raisanen, J., et al.: Glucose metabolism via the pentose phosphate pathway, glycolysis and Krebs cycle in an orthotopic mouse model of human brain tumors. NMR Biomed. **25**, 1177–1186 (2012)
26. Marin-Valencia, I., Yang, C., Mashimo, T., Cho, S., Baek, H., Yang, X.L., Rajagopalan, K.N., Maddie, M., Vemireddy, V., Zhao, Z., et al.: Analysis of tumor metabolism reveals mitochondrial glucose oxidation in genetically diverse human glioblastomas in the mouse brain in vivo. Cell Metab. **15**, 827–837 (2012)
27. Yang, C., Harrison, C., Jin, E.S., Chuang, D.T., Sherry, A.D., Malloy, C.R., Merritt, M.E., DeBerardinis, R.J.: Simultaneous steady-state and dynamic 13C NMR can differentiate alternative routes of pyruvate metabolism in living cancer cells. J. Biol. Chem. **289**, 6212–6224 (2014)
28. Burgess, S.C., Hausler, N., Merritt, M., Jeffrey, F.M., Storey, C., Milde, A., Koshy, S., Lindner, J., Magnuson, M.A., Malloy, C.R., et al.: Impaired tricarboxylic acid cycle activity in mouse livers lacking cytosolic phosphoenolpyruvate carboxykinase. J. Biol. Chem. **279**, 48941–48949 (2004)
29. Merritt, M.E., Harrison, C., Sherry, A.D., Malloy, C.R., Burgess, S.C.: Flux through hepatic pyruvate carboxylase and phosphoenolpyruvate carboxykinase detected by hyperpolarized 13C magnetic resonance. Proc. Natl. Acad. Sci. U. S. A. **108**, 19084–19089 (2011)
30. Fernandez, C.A., Des Rosiers, C.: Modeling of liver citric acid cycle and gluconeogenesis based on 13C mass isotopomer distribution analysis of intermediates. J. Biol. Chem. **270**, 10037–10042 (1995)
31. Katz, J.: Determination of gluconeogenesis in vivo with 14C-labeled substrates. Am. J. Phys. **248**, R391–R399 (1985)
32. Williamson, J.R., Walajtys-Rode, E., Coll, K.E.: Effects of branched chain alpha-ketoacids on the metabolism of isolated rat liver cells. I. Regulation of branched chain alpha-ketoacid metabolism. J. Biol. Chem. **254**, 11511–11520 (1979)
33. Moreno, K.X., Moore, C.L., Burgess, S.C., Sherry, A.D., Malloy, C.R., Merritt, M.E.: Production of hyperpolarized (13)CO2 from [1-(13)C]pyruvate in perfused liver does reflect total anaplerosis but is not a reliable biomarker of glucose production. Metabolomics. **11**, 1144–1156 (2015)
34. Lee, P., Leong, W., Tan, T., Lim, M., Han, W., Radda, G.K.: In vivo hyperpolarized carbon-13 magnetic resonance spectroscopy reveals increased pyruvate carboxylase flux in an insulin-resistant mouse model. Hepatology. **57**, 515–524 (2013)
35. Jin, E.S., Moreno, K.X., Wang, J.X., Fidelino, L., Merritt, M.E., Sherry, A.D., Malloy, C.R.: Metabolism of hyperpolarized [1-(13)C]pyruvate through alternate pathways in rat liver. NMR Biomed. **29**, 466–474 (2016)
36. Holyoak, T., Sullivan, S.M., Nowak, T.: Structural insights into the mechanism of PEPCK catalysis. Biochemistry. **45**, 8254–8263 (2006)
37. Sullivan, S.M., Holyoak, T.: Structures of rat cytosolic PEPCK: insight into the mechanism of phosphorylation and decarboxylation of oxaloacetic acid. Biochemistry. **46**, 10078–10088 (2007)

38. Keshari, K.R., Wilson, D.M.: Chemistry and biochemistry of 13C hyperpolarized magnetic resonance using dynamic nuclear polarization. Chem. Soc. Rev. **43**, 1627–1659 (2014)
39. Meier, S., Jensen, P.R., Duus, J.O.: Real-time detection of central carbon metabolism in living Escherichia coli and its response to perturbations. FEBS Lett. **585**, 3133–3138 (2011)
40. Jensen, P.R., Karlsson, M., Lerche, M.H., Meier, S.: Real-time DNP NMR observations of acetic acid uptake, intracellular acidification, and of consequences for glycolysis and alcoholic fermentation in yeast. Chemistry. **19**, 13288–13293 (2013)
41. Meier, S., Karlsson, M., Jensen, P.R., Lerche, M.H., Duus, J.O.: Metabolic pathway visualization in living yeast by DNP-NMR. Mol. BioSyst. **7**, 2834–2836 (2011)
42. Timm, K.N., Hartl, J., Keller, M.A., Hu, D.E., Kettunen, M.I., Rodrigues, T.B., Ralser, M., Brindle, K.M.: Hyperpolarized [U-(2) H, U-(13) C]glucose reports on glycolytic and pentose phosphate pathway activity in EL4 tumors and glycolytic activity in yeast cells. Magn. Reson. Med. **74**, 1543–1547 (2015)
43. Harris, T., Degani, H., Frydman, L.: Hyperpolarized 13C NMR studies of glucose metabolism in living breast cancer cell cultures. NMR Biomed. **26**, 1831–1843 (2013)
44. Rodrigues, T.B., Serrao, E.M., Kennedy, B.W., Hu, D.E., Kettunen, M.I., Brindle, K.M.: Magnetic resonance imaging of tumor glycolysis using hyperpolarized 13C-labeled glucose. Nat. Med. **20**, 93–97 (2014)
45. Teusink, B., Passarge, J., Reijenga, C.A., Esgalhado, E., van der Weijden, C.C., Schepper, M., Walsh, M.C., Bakker, B.M., van Dam, K., Westerhoff, H.V., et al.: Can yeast glycolysis be understood in terms of in vitro kinetics of the constituent enzymes? Testing biochemistry. Eur. J. Biochem. **267**, 5313–5329 (2000)
46. Funk, A.M., Anderson, B.L., Wen, X., Hever, T., Khemtong, C., Kovacs, Z., Sherry, A.D., Malloy, C.R.: The rate of lactate production from glucose in hearts is not altered by per-deuteration of glucose. J. Magn. Reson. **284**, 86–93 (2017)
47. Mishkovsky, M., Anderson, B., Karlsson, M., Lerche, M.H., Sherry, A.D., Gruetter, R., Kovacs, Z., Comment, A.: Measuring glucose cerebral metabolism in the healthy mouse using hyperpolarized (13)C magnetic resonance. Sci. Rep. **7**, 11719 (2017)
48. Park, J.M., Wu, M., Datta, K., Liu, S.C., Castillo, A., Lough, H., Spielman, D.M., Billingsley, K.L.: Hyperpolarized sodium [1-(13)C]-Glycerate as a probe for assessing glycolysis in vivo. J. Am. Chem. Soc. **139**, 6629–6634 (2017)
49. Moreno, K.X., Satapati, S., DeBerardinis, R.J., Burgess, S.C., Malloy, C.R., Merritt, M.E.: Real-time detection of hepatic gluconeogenic and glycogenolytic states using hyperpolarized [2-13C]dihydroxyacetone. J. Biol. Chem. **289**, 35859–35867 (2014)
50. Jin, E.S., Lee, M.H., Murphy, R.E., Malloy, C.R.: Pentose phosphate pathway activity parallels lipogenesis but not antioxidant processes in rat liver. Am. J. Physiol. Endocrinol. Metab. **314**, E543–E551 (2018)
51. Moreno, K.X., Harrison, C.E., Merritt, M.E., Kovacs, Z., Malloy, C.R., Sherry, A.D.: Hyperpolarized delta-[1-(13) C]gluconolactone as a probe of the pentose phosphate pathway. NMR Biomed. **30**, e3713 (2017)

Further Reading

Chaumeil, M.M., Radoul, M., Najac, C., Eriksson, P., Viswanath, P., Blough, M.D., Chesnelong, C., Artee Luchman, H., Gregory Cairncross, J., Ronen, S.M.: Hyperpolarized ^{13}C MR imaging detects no lactate production in mutant IDH1 gliomas: Implications for diagnosis and response monitoring. NeuroImage Clin. **12**, 180–189 (2016)

Comment, A., Merritt, M.E.: Hyperpolarized magnetic resonance as a sensitive detector of metabolic function. Biochemistry. **53**, 7333–7357 (2014)

Hesketh, R.L., Brindle, K.M.: Magnetic resonance imaging of cancer metabolism with hyperpolarized ^{13}C-labeled cell metabolites. Curr. Opin. Chem. Biol. **45**, 187–194 (2018)